Earthquakes triggered by fluid extraction

P. Segall
U.S. Geological Survey, Menlo Park, California 94025
and Department of Geophysics, Stanford University, Stanford, California 94305-2215

ABSTRACT

Seismicity is correlated in space and time with production from some oil and gas fields where pore pressures have *declined* by several tens of megapascals. Reverse faulting has occurred both above and below petroleum reservoirs, and normal faulting has occurred on the flanks of at least one reservoir. The theory of poroelasticity requires that fluid extraction locally alter the state of stress. Calculations with simple geometries predict stress perturbations that are consistent with observed earthquake locations and focal mechanisms. Measurements of surface displacement and strain, pore pressure, stress, and poroelastic rock properties in such areas could be used to test theoretical predictions and improve our understanding of earthquake mechanics.

INTRODUCTION

Earthquakes induced by injection of fluids into the subsurface are thought to result from increased pore pressures that decrease effective normal stresses and allow faults to slip at ambient levels of shear stress (Healy et al., 1968; Raleigh et al., 1972, 1976). It may thus seem paradoxical that faulting and seismicity have also been attributed to fluid extraction in a number of localities. Because fluid extraction decreases pore pressure, the same argument suggests that extraction should increase the effective confining stress and inhibit fault slip. Yet the evidence for extraction-induced seismicity is compelling (Yerkes and Castle, 1976), and this apparent paradox requires an explanation. I review here the characteristics of earthquakes induced by subsurface fluid extraction and discuss a quantitative model to explain the phenomenon. A field experiment to test the validity of the theory is proposed.

OBSERVATIONS

During the 1920s, series of earthquakes were felt near the Goose Creek oil field in south Texas. Oil production there caused the field to subside by as much as 1 m between 1917 and 1925 (Pratt and Johnson, 1926). The earthquakes occurred on normal faults that broke the surface along the northern and southern margins of the subsiding region. Recurrent slip on these faults dropped the oil field relative to the surroundings by as much as 0.4 m. Fault slip was accompanied by "slight earthquakes which shook houses, displaced dishes, spilled water, and disturbed the inhabitants generally" (Pratt and Johnson, 1926).

Seismicity and spectacular surface deformation accompanied oil production from the Wilmington oil field in Long Beach, California. Subsidence between 1936 and 1966 reached 9 m; horizontal displacements were as large as 3.7 m. A profile of the horizontal strain (Fig. 1) shows that the central subsiding region contracted as much as 1.2%, whereas the flanks of the subsiding region extended by a few tenths of one percent. To put this in perspective, these strain rates were more than one thousand times greater than strain rates observed along locked sections of the San Andreas fault. Six shallow earthquakes (M 2.4 to 3.3) occurred within the oil field between 1947 and 1955, when the rate of subsidence was greatest (Kovach, 1974). The earthquakes were generated by slip on bedding planes at depths of 470 to 520 m, which sheared off tens to hundreds of wells over several square kilometres (Kovach, 1974). Virtually all of the compaction that caused the surface subsidence was localized in the producing beds at depths of 650 to 1050 m (Allen and Mayuga, 1970), several

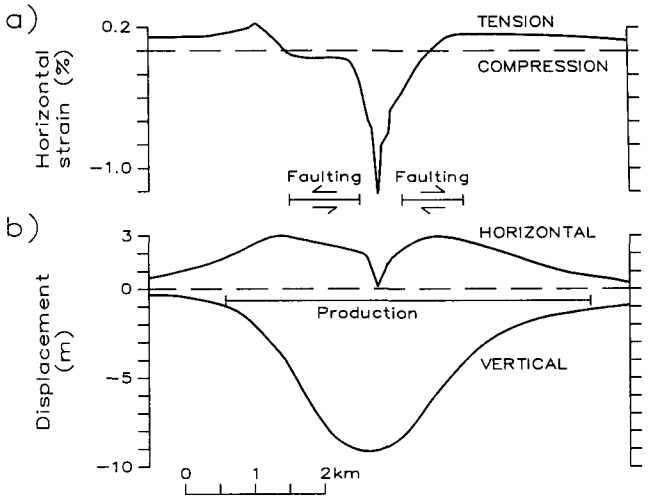

Figure 1. Measured surface deformation at Wilmington oil field near Long Beach, California. Top: Horizontal strain change. Bottom: Radial displacement (inward positive) between 1937 and 1962, and vertical displacement (downward negative) between 1928 and 1962. Also shown are limits of producing zone and location of bedding plane faults. After Yerkes and Castle (1970).

hundred metres below the slip surfaces. The faults were located near the center of subsidence (Fig. 1) within the area that contracted horizontally at the Earth's surface (Kovach, 1974; Yerkes and Castle, 1976).

Active, aseismic reverse faulting has been recognized within the Buena Vista Hills oil field, California, for several decades (Koch, 1933). The 2.6-km-long Buena Vista Hills fault dips 25°N and slipped at a rate of ~2 cm/yr between 1932 and 1967 (Nason et al., 1968). Slip on the fault sheared wells, produced a surficial scarp, and buckled oil, gas, and water pipelines. The fault is located in a region of substantial subsidence (maximum of 2.3 m between 1942 and 1964) and horizontal contraction (strain rates of 10^{-5}/yr between 1932 and 1959; Whitten, 1961; Howard, 1968). Although the western margin of the San Joaquin valley is known to be tectonically active, the extreme horizontal strain and local subsidence suggest that fluid withdrawal is a significant factor in the faulting.

The Rocky Mountain House seismic zone in Alberta, Canada, is the most seismically active region in Alberta and is located near several major gas fields (Wetmiller, 1986). Gas production from lower Paleozoic carbonates at depths of 3 to 5 km began in 1971. Prior to 1976 there were only two earthquakes located by the regional network (Fig. 2a). By 1976 the average reservoir pressure had dropped by 25 MPa and the rate of seismicity ($M \leq 3.4$) had increased dramatically. Wetmiller (1986) used a local seismic network to obtain improved hypocenters and to better define the association of the gas fields with the seismicity. He found that all of the 67 events located during the experiment occurred within a 5-km-diameter by 1-km-thick zone located immediately below the Strachan pool (Fig. 3). A composite focal mechanism indicated reverse faulting with nearly horizontal, east-west–trending P-axis (Wetmiller, 1986).

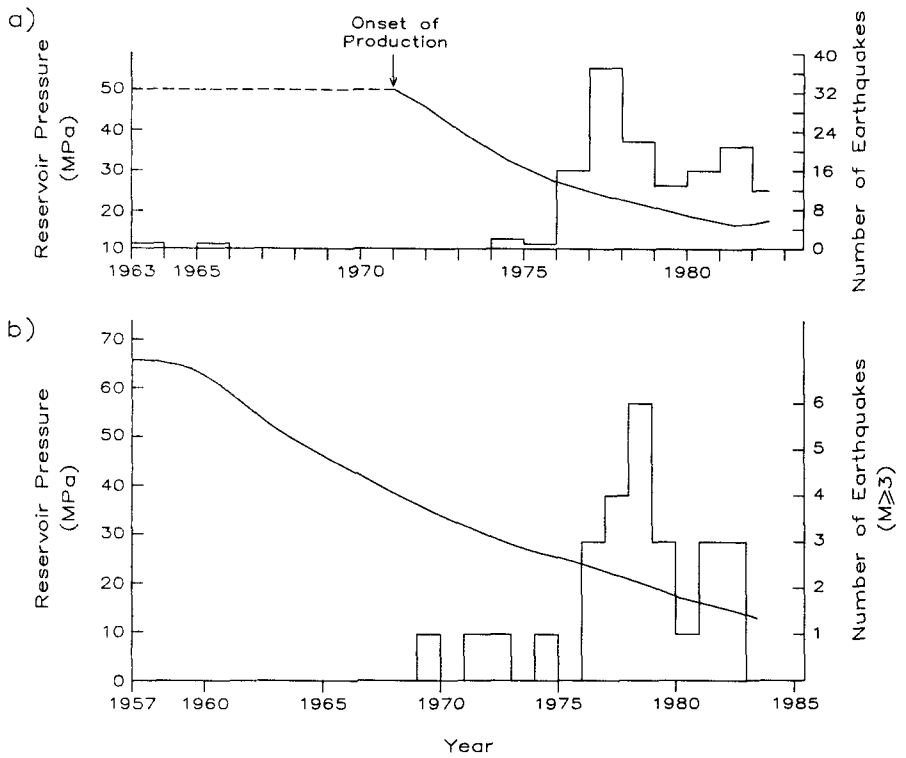

Figure 2. Number of earthquakes recorded per year and decline in average reservoir pressure in two gas fields. a: Strachan field in Alberta, Canada. Earthquakes recorded by Canadian regional network (Wetmiller, 1986). Average static bottom-hole pressure at 2.8 km depth provided by R. J. Wetmiller (1985, written commun.). b: Pau basin, France. M ≥3 earthquakes and average reservoir pressure (after Grasso and Wittlinger, 1989).

Grasso and Wittlinger (1989) recorded nearly 800 earthquakes with magnitudes up to 4.2 clustering in a small volume around an active gas field in the Pau basin in the foreland of the western Pyrenees. These earthquakes are separated by 25 km from, and are shallower than, regional Pyrenean seismicity. The gas reservoir is a 500-m-thick sequence of Cretaceous and Upper Jurassic limestones that forms a broad anticline at depths of 3.2 to 5.5 km. The pore pressure in the reservoir has decreased by 50 MPa since the onset of exploitation (Fig. 2b). Earthquakes began in 1969 when the reservoir pressure had decreased by ~30 MPa. Repeated leveling shows maximum subsidence of only ~5 cm between 1887 and 1967 (Grasso and Feignier, 1989). Grasso and Wittlinger (1989) found that 95% of the well-located events and all the M > 3 events have epicenters within the boundaries of the gas field. Most events are shallow, having focal depths of 2.5 to 5.0 km. More than 85% of the better located events are concentrated near the top of the gas reservoir; less than 10% are located within the reservoir itself (Grasso and Feignier, 1989). Composite focal mechanisms constructed from clusters of events suggest that P-axes are subhorizontal and crudely radially distributed (Grasso and Feignier, 1989).

Seismicity is associated with fluid extraction in a number of other areas. Pennington et al. (1986) showed that earthquakes as large as M 3.9 have clustered near the Imogene oil field and the Fashing gas field in south Texas, where reservoir pressures have declined by 10 MPa and 22 MPa, respectively. Simpson and Leith (1985) discussed the possible association of three m_s 7.0 earthquakes with a major gas field at Gazli in Soviet Uzbekistan. Yerkes and Castle (1970, 1976) summarized other earthquakes and ground faulting related to fluid extraction.

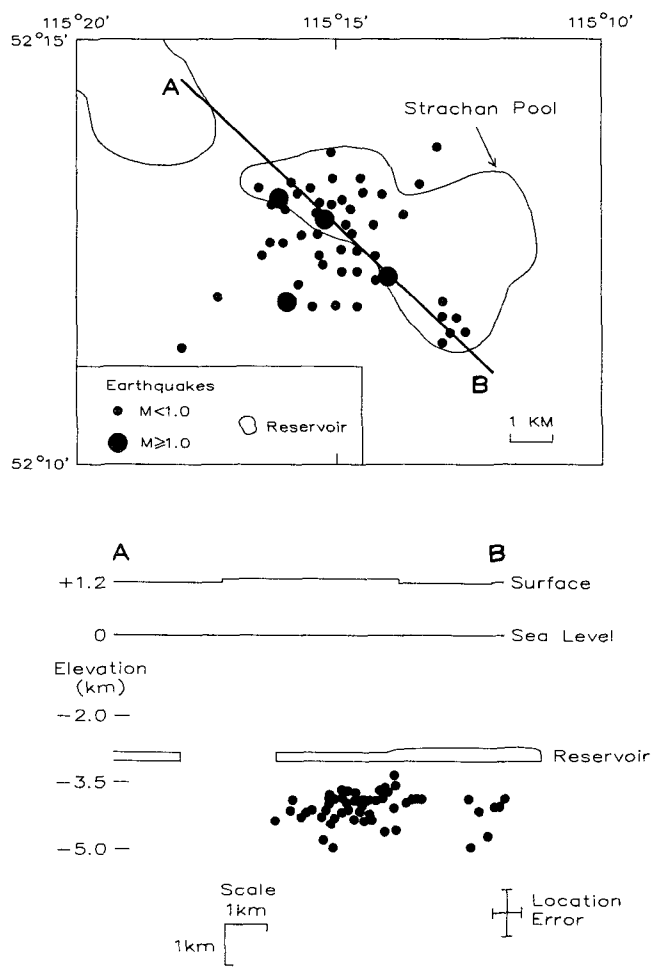

Figure 3. Map and cross section of microseismicity showing earthquakes clustered 1 to 2 km beneath Strachan field, Alberta, Canada. Earthquakes located by local network in 1980 (from Wetmiller, 1986).

The observations are summarized in the schematic cross section of Figure 4. Extraction of pore fluids causes subsidence, with accompanying horizontal contraction of the center of the subsiding region and lesser extension of the flanks. Both normal and reverse faults may accompany extraction. As at the Goose Creek field, normal faults may develop at the margins of the subsiding region. Reverse faults form in the central contracting region. At Wilmington, Buena Vista Hills, and Pau, the reverse faulting is localized above the producing layers. At Rocky Mountain House, the seismicity is below the reservoir.

THEORY

A variety of models have been proposed to account for the earthquakes in these various localities (see respective references). I suggest that all the observations described in the previous section can be understood by considering the stress changes caused by fluid extraction.

The constitutive equations for a linear poroelastic medium are

$$2\mu\epsilon_{ij} = \sigma_{ij} - \frac{\nu}{1+\nu}\sigma_{kk}\delta_{ij} + \frac{(1-2\nu)\alpha}{1+\nu}p\delta_{ij}, \tag{1a}$$

and

$$\Delta m = \frac{(1-2\nu)\alpha\rho_o}{2\mu(1+\nu)}\left[\sigma_{kk} + \frac{3}{B}p\right] \tag{1b}$$

(Biot, 1941; Rice and Cleary, 1976). Equation 1a relates the strain ϵ_{ij} to the stress acting on the material element σ_{ij} and the pore pressure p. Equation 1b relates the change in fluid mass per unit volume (Δm) to σ_{kk} and p, where $m = \rho\nu$, ρ is the fluid density (ρ_o in the reference state), and ν is the fluid volume fraction.

There are four material constants in equation 1: the shear modulus μ, Poisson's ratio ν, Skempton's coefficient B, and α. The constant α is related to the bulk moduli of the saturated rock (K) and the grains in the rock (K_s) by $\alpha = 1 - K/K_s$ (Nur and Byerlee, 1971). Skempton's coefficient B is the ratio of induced pore pressure to confining stress under "undrained" (no flow) conditions (equation 1b gives $p = -B\sigma_{kk}/3$ when $\Delta m = 0$). If the porosity forms a continuous network, then $B = \alpha[\alpha + \nu_o(K/K_f - K/K_s)]^{-1}$, where K_f is the bulk modulus of the fluid (Rice and Cleary, 1976). If the rock is much more compressible than the grains ($K << K_s$), then $\alpha \sim 1$. If in addition, $K << K_f$, then $B \sim 1$.

To understand deformation induced by fluid extraction, it is useful to use equation 1b to write the strain in terms of Δm. The volume strain is

$$\epsilon_{kk} = \frac{\sigma_{kk}}{3K_u} + \frac{B\Delta m}{\rho_o}. \tag{2}$$

Equation 2 has a simple and important physical interpretation. It states that the volume strain (ϵ_{kk}) is composed of two parts: an elastic component under conditions of no pore-fluid flow $\sigma_{kk}/3K_u$ (where K_u is the undrained bulk modulus), and a component resulting from changes in the amount of fluid in the pores of the rock $B\Delta m/\rho_o$. Extraction of pore fluids results in localized contraction of the reservoir rocks, stressing and deforming the surrounding rock mass.

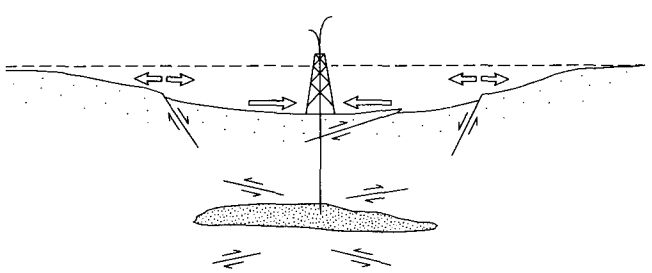

Figure 4. Schematic cross section summarizing surface deformation and faulting associated with fluid withdrawal. Open arrows indicate horizontal strain at Earth's surface. Normal faults develop on flanks of field, as at Goose Creek field. Reverse faulting occurred above reservoirs at Wilmington, Buena Vista Hills, and Pau, and below reservoir at Strachan field (see Fig. 3).

The form of the governing equations, which express stress equilibrium and continuity of pore-fluid mass, depends on the choice of free variables. The appropriate choice of variables depends on the boundary conditions and, to some degree, on the available data. Adopting displacement u_i and pore-fluid mass Δm as the free variables, we have

$$\mu\nabla^2 u_i + \frac{\mu}{(1-2\nu_u)}\frac{\partial^2 u_j}{\partial x_i \partial x_j} - \frac{BK_u}{\rho_o}\frac{\partial \Delta m}{\partial x_i} = 0, \tag{3}$$

and

$$c\nabla^2(\Delta m) = \frac{\partial(\Delta m)}{\partial t} \tag{4}$$

(Segall, 1985), where ν_u is the undrained Poisson's ratio, and c is the hydraulic diffusivity of the medium.

If fluid production is from permeable layers imbedded in relatively impermeable surroundings, then $\Delta m \sim 0$ outside the producing zone. Given the net flux of fluid out of the reservoir it is possible to solve for $\Delta m(\mathbf{x}, t)$ from equation 4 and to use equation 3 to calculate the displacements and stress (Segall, 1985). In contrast, choosing p and σ_{ij} as variables results in coupled equilibrium and diffusion equations that, in general, must be solved simultaneously (Rice and Cleary, 1976). Previously, Geertsma (1966, 1973) computed displacements and stresses for a uniform pressure decrease in a thin disk-shaped reservoir, although he did not apply this to induced seismicity. Kosloff et al. (1980a, 1980b) conducted finite element simulations of the Wilmington subsidence, taking measured pressure changes as input, and calculated stress changes on the fault planes. Note that because of the mechanical coupling between stress and pore pressure, there are undrained pore-pressure changes outside the reservoir, even when there are no changes in fluid content at those points.

Assuming that $\Delta m(\mathbf{x}, t)$ are found from equation 4, the displacements and stresses can be calculated from

$$\mu u_i(\mathbf{x},t) = \frac{\mu(1+\nu_u)B}{3(1-\nu_u)\pi\rho_o}\int_V \Delta m(\zeta,t) g_i(\mathbf{x},\zeta)\, dV_\zeta, \tag{5}$$

and

$$\sigma_{ij}(\mathbf{x},t) = \frac{\mu(1+\nu_u)B}{3(1-\nu_u)\pi\rho_o}\left[\int_V \Delta m(\zeta,t) G_{ij}(\mathbf{x},\zeta)\, dV_\zeta - \Delta m(\mathbf{x},t)\right]. \tag{6}$$

The integration is over the volume for which $\Delta m \neq 0$. The Green's functions $g_i(\mathbf{x}, \zeta)$ and $G_{ij}(\mathbf{x}, \zeta)$ are equivalent to unit point centers of dilatation (Geertsma, 1973; Segall, 1985). If $p(\mathbf{x},t)$ is the variable, a similar result holds if the integration is taken over the entire volume for which $p \neq 0$, and the constant factor is replaced by $\alpha(1-2\nu)/2\pi(1-\nu)$.

The important result is that stresses are generated where there are no changes in pore-fluid content. From equation 6, σ_{ij} at $\mathbf{x}$ is, in general, nonzero when Δm at $\mathbf{x}$ vanishes. Moreover, in the following section we see that the distribution of these stresses is consistent with earthquakes occurring near zones of fluid depletion. The stresses, unlike the displacements, scale with μ, so that if the rock is stiff, large stresses may be generated without massive subsidence. Finally, note that stress changes caused by reduction in gravitational load are *not* included here. The stresses are roughly one-thousandth of the poroelastic stresses discussed here and are safely neglected (Segall, 1985).

COMPARISON OF PREDICTIONS AND OBSERVATIONS

As a simple example to illustrate the basic physical process, consider the stress and deformation resulting from the withdrawal of fluid from a flat permeable layer of thickness, T, small compared to the depth, D, embedded in an otherwise impermeable half-space (Fig. 5, inset). For simplicity, we take $\Delta m(t)$ to be uniform over the interval $-a < y < a$ and

assume plane-strain conditions (no strain in the z direction). The surface displacements and strains are found, using the plane-strain Green's functions given in Segall (1985, Appendix C), to be

$$u_x(x = 0,y,t) = \frac{2(1 + \nu_u)BT\Delta m(t)}{3\pi\rho_0}\left[\tan^{-1}(\xi_-) - \tan^{-1}(\xi_+)\right], \quad (7a)$$

$$u_y(x = 0,y,t) = \frac{2(1 + \nu_u)BT\Delta m(t)}{6\pi\rho_0}\log\left[\frac{1 + \xi_+^2}{1 - \xi_-^2}\right] \quad (7b)$$

and

$$\epsilon_{yy}(x = 0,y,t) = \frac{2(1 + \nu_u)BT\Delta m(t)}{3\pi\rho_0 D}\left[\frac{\xi_+}{1 + \xi_+^2} - \frac{\xi_-}{1 + \xi_-^2}\right], \quad (7c)$$

where $\xi_- = (y - a)/D$ and $\xi_+ = (y + a)/D$. These are shown in Figure 5 for $\Delta m < 0$ (fluid extraction) and $a/D = 1.0$. The vertical displacements u_x show broad subsidence, whereas the horizontal strains ϵ_{yy} are negative (contraction) over the field and positive (extension) on the flanks of the field, both consistent with the observations (Fig. 1). From equation 7, the ratio of the maximum subsidence to maximum horizontal strain (for $a/D = 1.0$) is $D\pi/2$. At Wilmington, the peak subsidence and horizontal strain were of the order of 10 m and 10^{-2}, respectively. This would suggest that $D \sim 10^3$ m, consistent with the actual reservoir depth of 600 to 1000 m.

The change in horizontal stress σ_{yy} and the orientation of the planes of maximum shear are shown in Figure 6. The rock above and below the producing layer is compressed horizontally, whereas the rock on the flanks goes through relative tension (or decrease in compression). Significant stress changes extend both above and below the producing layer.

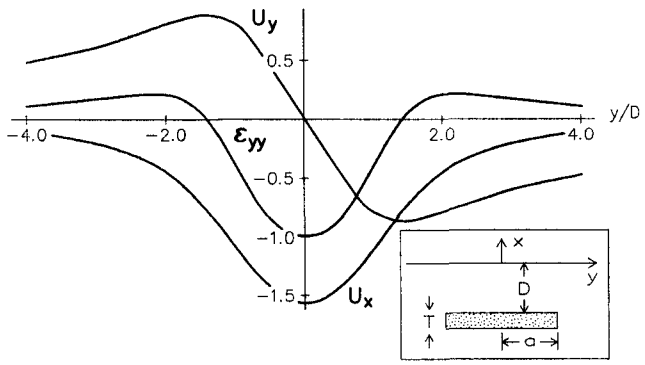

Figure 5. Calculated surface displacements u_x, u_y, and strain ϵ_{yy} (extension positive) for $a/D = 1.0$. Geometry is shown in inset. Displacements are normalized by $2(1 + \nu_u)\,BT\Delta m(t)/3\pi\rho_0 D$, strains by $2(1 + \nu_u)\,BT\Delta m(t)/3\pi\rho_0 D$.

Faults slip when the total shear stress (the sum of the ambient and induced stresses) overcomes the frictional resistance. Favored slip planes therefore depend on the orientation and magnitude of the ambient stress. Because this presumably varies from site to site, I consider here only the component of stress induced by extraction. Furthermore, because the induced normal stresses are largely balanced by undrained pore-pressure changes, the frictional resistance does not change much and we can focus on the changes in shear stress. The orientation of the planes of maximum shear, as shown by the simulated focal mechanisms in Figure 6, predict reverse faulting above and below the producing zone and normal faulting on the flanks of the producing zone. These results are qualitatively consistent with the location and orientation of the faulting at Goose Creek, Wilmington, Buena Vista Hills, Alberta, and Pau as summarized in Figure 4. Note that the substantial decrease in pressure within the reservoir inhibits frictional slip within the reservoir rocks themselves.

The stress pattern shown in Figure 6 can be understood in a straightforward manner. Fluid extraction causes the reservoir rock to contract. Contraction in the vertical direction is accommodated by subsidence of the free surface. Contraction in the horizontal direction, on the other hand, is resisted by the surrounding rocks, which are pulled in toward the center of the reservoir. This causes the strata above and below the reservoir to be driven into horizontal compression. Rock far away from the reservoir is displaced less than rock immediately above and below the reservoir, causing the flanking regions to extend.

PROPOSED EXPERIMENT

The theory is testable, allowing the horizontal and vertical displacement, pore pressure, and stress to be calculated given the mass flux of fluid from the reservoir and appropriate material properties. These fields can also be measured in situ. In particular, it may be possible to record the change in total stress by repeated hydraulic fracturing, perhaps reopening the same fracture at different times. Surface displacements can be measured with either conventional techniques (leveling and trilateration) or with the Global Positioning System (GPS).

Will the changes be large enough to measure unambiguously? Pore-pressure changes (typically tens of megapascals) are easily monitored. Vertical displacements (subsidence) range from metres above shallow reservoirs in poorly consolidated materials to centimetres above deeper

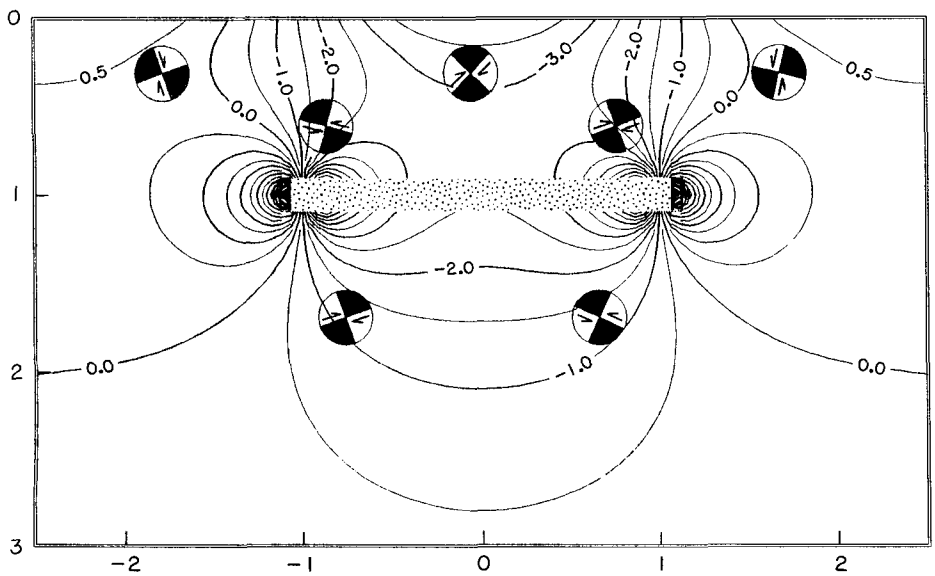

Figure 6. Calculated change in horizontal normal stress σ_{yy} due to fluid extraction (relative tension positive). Stress is not contoured in producing zone ($x = D$, $-a < y < a$. Simulated focal mechanisms indicate planes of maximum shear stress, and sense of shear on those planes (compare with Fig. 4). Horizontal distance and depth in units of reservoir depth D. Stress contoured in units of $\mu(1 + \nu_u) \cdot BT\Delta m(t)/3\pi\rho_0 D(1 - \nu_u)$.

reservoirs in well-lithified materials. Horizontal displacements are comparable to the vertical displacements. We can make order-of-magnitude estimates of the expected stress changes by using the linear poroelastic model. If we assume $\alpha (1 - 2\nu)/2\pi(1 - \nu) \sim 0.1$ and $T/D \sim 0.1$, then the stress changes are $\sigma_{ij} \sim 0.01 \times p \times F_{ij} (x/D, y/D, a/D)$. Here $F_{ij} (x/D, y/D, a/D)$ is a dimensionless function of position and reservoir geometry; a typical value directly above the reservoir (for $a/D = 1$ from Fig. 6) is $F_{yy} \sim 3$. Thus, a pressure decrease of 35 MPa (Fig. 2) gives stress changes of the order of 1 MPa (10 bar). Abrupt gradients in p or Δm cause stress concentrations that are even larger than this (Fig. 6).

The ratio of maximum surface strain to subsidence is $\epsilon_{yy} (0,0)/u_x (0,0) \sim 2/\pi D$. Because Hooke's law at the free surface reduces to $\sigma_{yy} (x = 0) = 2\mu\epsilon_{yy} (x = 0)/(1 - \nu_u)$, the ratio of stress change to subsidence is $\sim 4\mu/(1 - \nu_u)D\pi$. For $\nu_u \sim 1/3$, the ratio is $\sim 2\mu/D$. Taking $D = 2$ km and $\mu = 10^4$ MPa, we can anticipate stress changes of ~0.1 MPa per centimetre of subsidence. Thus, extraction from deeper, well-lithified strata can produce measurable stress changes with only modest amounts of surface subsidence. For example, the ~5 cm of subsidence observed in Pau would correspond to stress changes of ~0.5 MPa (5 bar), reasonably consistent with the estimate based on the reservoir pressure change.

It should be possible to measure displacements, stress, and pore-pressure changes associated with extraction. With laboratory measurements of the appropriate physical properties, it should also be possible to make independent theoretical estimates of these quantities and to compare them to the field measurements as well as the distribution and orientation of induced earthquakes.

DISCUSSION

Poroelastic stresses caused by changes in the distribution of pore fluids are likely to be important in other settings. Such stress changes must have accompanied fluid injection at the Rocky Mountain Arsenal near Denver (Healy et al., 1968) and at Rangely, Colorado (Raleigh et al., 1972, 1976). The role of poroelastic stressing in these cases of induced seismicity is more difficult to establish because large pore-pressure increases are themselves destabilizing, whereas the large pore-pressure decreases accompanying extraction are inherently stabilizing.

It is possible that poroelastic stressing could be used in active studies of earthquake mechanics. It should be possible to extend the kind of experiment performed at Rangely, Colorado (Raleigh et al., 1976), and use stresses induced by fluid extraction to study the earthquake generation process in situ. Given a region with well-characterized hydraulic and mechanical properties, it should be possible to modify the stress and stress rate in a controlled fashion. Monitoring the resulting seismicity would help test slip-instability models such as slip weakening and slip rate and state-dependent friction that predict different behavior for different loading histories. Such experiments could present a way to test models based on laboratory experiments using faults in the Earth at scales up to several kilometres.

REFERENCES CITED

Allen, D.R., and Mayuga, M.N., 1970, The mechanics of compaction and rebound, Wilmington oil field, Long Beach, California, U.S.A., *in* Land subsidence: International Association of the Science of Hydrology, UNESCO Publication 89, v. 2, p. 410–423.

Biot, M.A., 1941, General theory of 3-dimensional consolidation: Journal of Applied Physics, v. 12, p. 155–164.

Geertsma, J., 1966, Problems of rock mechanics in petroleum production engineering, *in* Proceedings, First Congress International Society of Rock Mechanics, Lisbon: Lisbon, Labatorio Nacional de Engenharia Civil, p. 585–594.

——1973, Land subsidence above compacting oil and gas reservoirs: Journal of Petroleum Technology, v. 25, p. 734–744.

Grasso, J.R., and Feignier, B., 1989, Mechanical behaviour and structural evolution induced by a depletion: A case study of a gas field, *in* Proceedings, Second International Symposium on Rockbursts and Seismicity in Mines, Minneapolis, Minnesota, June 8–10, 1988: Rotterdam, the Netherlands, Balkema (in press).

Grasso, J.R., and Wittlinger, G., 1989, 10 years of seismic monitoring over a gas field area: Seismological Society of America Bulletin (in press).

Healy, J.H., Rubey, W.W., Griggs, D.T., and Raleigh, C.B., 1968, The Denver earthquakes: Science, v. 161, p. 1301–1310.

Howard, J.H., 1968, Recent deformation at Buena Vista Hills, California: American Journal of Science, v. 266, p. 737–757.

Koch, T.W., 1933, Analysis and effects of current movements on an active fault in Buena Vista Hills oil field, Kern County, California: American Association of Petroleum Geologists Bulletin, v. 17, p. 694–712.

Kosloff, D., Scott, R.F., and Scranton, J., 1980a, Finite element simulation of Wilmington oil field subsidence: I. Linear modeling: Tectonophysics, v. 65, p. 339–368.

——1980b, Finite element simulation of Wilmington oil field subsidence: II. Nonlinear modeling: Tectonophysics, v. 70, p. 159–183.

Kovach, R.L., 1974, Source mechanisms for Wilmington oil field, California, subsidence earthquakes: Seismological Society of America Bulletin, v. 64, no. 3, pt. 1, p. 699–711.

Nason, R.D., Cooper, A.K., and Tocher, D., 1968, Slippage on the Buena Vista thrust fault, *in* Geology and oil fields, west side southern San Joaquin valley (43rd annual meeting guidebook, AAPG, SEG, SEPM, Pacific sections): Los Angeles, California, American Association of Petroleum Geologists, Pacific Section, p. 100–101.

Nur, A., and Byerlee, J.D., 1971, An exact effective stress law for elastic deformation of rock with fluids: Journal of Geophysical Research, v. 76, p. 6414–6419.

Pennington, W.D., Davis, S.D., Carlson, S.M., DuPree, J.D., and Ewing, T.E., 1986, The evolution of seismic barriers and asperities caused by the depressuring of fault planes in oil and gas fields of south Texas: Seismological Society of America Bulletin, v. 76, p. 939–948.

Pratt, W.E., and Johnson, D.W., 1926, Local subsidence of the Goose Creek oil field: Journal of Geology, v. 34, pt. 1, p. 577–590.

Raleigh, C.B., Healy, J.H., and Bredehoeft, J.D., 1972, Faulting and crustal stress at Rangely, Colorado, *in* Heard, H.C., Borg, I.Y., Carter, N.L., and Raleigh, C.B., eds., Flow and fracture of rocks (Griggs volume): American Geophysical Union Geophysical Monograph 16, p. 275–284.

——1976, An experiment in earthquake control at Rangely, Colorado: Science, v. 191, p. 1230–1237.

Rice, J.R., and Cleary, M.P., 1976, Some basic stress diffusion solutions for fluid-saturated elastic porous media with compressible constituents: Reviews of Geophysics and Space Physics, v. 14, p. 227–241.

Segall, Paul, 1985, Stress and subsidence resulting from subsurface fluid withdrawal in the epicentral region of the 1983 Coalinga earthquake: Journal of Geophysical Research, v. 90, p. 6801–6816.

Simpson, D.W., and Leith, W., 1985, The 1976 and 1984 Gazli, USSR, earthquakes—Were they induced?: Seismological Society of America Bulletin, v. 75, p. 1465–1468.

——1976, Seismicity and faulting attributable to fluid extraction: Engineering Geology, v. 10, p. 151–167.

Wetmiller, R.J., 1986, Earthquakes near Rocky Mountain House, Alberta, and their relationship to gas production: Canadian Journal of Earth Sciences, v. 23, p. 172–181.

Whitten, C.A., 1961, Measurements of small movements of the earth's crust: Academiae Scientiarum Fennicae Annales, ser. A, III Geologica-Geographica, Suomalainen Tiedeakatimia, no. 61, p. 315–320.

Yerkes, R.F., and Castle, R.O., 1970, Surface deformation associated with oil and gas field operations in the United States, *in* Land subsidence: International Association of the Science of Hydrology, UNESCO Publication 89, v. 1, p. 55–66.

ACKNOWLEDGMENTS

I thank Bob Wetmiller, J.R. Grasso, and Bob Yerkes for data and insights on induced earthquakes, and John Rudnicki, Dave McTigue, Evelyn Roeloffs, and Jim Rice for discussions about poroelasticity. The manuscript was reviewed by Barry Raleigh, John Bredehoeft, Bob Simpson, and Evelyn Roeloffs.

Manuscript received March 27, 1989
Revised manuscript received May 30, 1989
Manuscript accepted June 16, 1989

Reviewer's comment

A classy piece of work on a fascinating subject.

C. Barry Raleigh